Swimming in circles of a Janus particle by diffusion of insoluble surfactant on its active face

Darren Crowdy *

Department of Mathematics, Imperial College London, 180 Queen's Gate, London SW7 2AZ, United Kingdom

(Received 6 November 2024; accepted 17 September 2025; published 15 October 2025)

An exact solution is obtained for the Stokes flow around an active circular two-dimensional Janus swimmer whose active face is a free surface and its inert face is a no-slip surface, a conceptual design motivated by recent work on superhydrophobic surfaces. Locomotion is driven by Marangoni stresses associated with the diffusion of insoluble surfactant from one edge of the active face to the other. The dynamical system governing the motion of the swimmer is derived explicitly in terms of the swimmer geometry. It is shown that this Marangoni-driven actuation mechanism results in a translational-rotational coupling causing the Janus particle to swim in circles while spinning about its center. While idealized, the model swimmer exemplifies a set of minimal ingredients needed to set up such translational-rotational coupling.

DOI: 10.1103/h36b-4ydh

I. INTRODUCTION

There has been considerable recent interest in the study of collective motion of active organisms, particles, and swimmers and their self-assembly into patterns, lattices, or other dynamically emergent structures [1–5]. Unlike those driven by external influences, active swimmers convert energy either stored onboard or extracted from the ambient fluid to sustain locomotion, often in low-Reynolds-number environments [1,2,6,7]. There are two main types: anisotropic which have an inherent asymmetry in their actuation mechanism, and isotropic swimmers, where the locomotion derives from an intrinsic nonlinearity in the coupled multiphysics transport dynamics [8]. A common example of an anisotropic swimmer is a so-called Janus particle characterized by two or more "faces" with contrasting physicochemical or biological properties; it is this two-facedness that produces the anisotropy. An important study of the use of phoretic flows to provide locomotion of Janus particles is due to Paxton *et al.* [9], who used colloidal rods with one end (or "face") platinum and the other gold; directed motion in an aqueous solution of hydrogen peroxide was caused by reaction at the platinum end of the rod. Much subsequent theoretical work to understand the dynamics of such Janus particles has since been done [1,6,7,10]. For example, a recent study [4] where the Marangoni effects caused by the presence of surfactants are important examines how the partitioning of oil between different compartments of a Janus droplet affects its swimming speed. A recent review of Janus micro/nanorobots in biomedical applications features a discussion of the diverse energy sources on which such robots rely, including those of a physical, chemical, and biological nature. The overriding aim of such studies is to understand how combinations of

*Contact author: d.crowdy@imperial.ac.uk

Published by the American Physical Society under the terms of the Creative Commons Attribution 4.0 International license. Further distribution of this work must maintain attribution to the author(s) and the published article's title, journal citation, and DOI.

multiphysics mechanisms can be used to design programmable microswimmers having desirable properties for applications.

The study of isolated active particles is a natural first step in understanding the more complicated scenarios of pairwise, and then multibody, interactions. In view of their coupled multiphysics nature with interplay between chemical and hydrodynamic effects, theoretical studies of isolated active particles driven by differing physical mechanisms in various settings have often focused on two-dimensional particles or droplets in order to gain fundamental behavioral insights while reducing the technical burden of a fully three-dimensional case. While theoretically attractive in this respect, the two-dimensional model also presents potential mathematical challenges: one is associated with the Stokes paradox of low-Reynolds-number hydrodynamics [11], and another with the divergence in the far field of a purely diffusive point source singularity often occurring when studying phoretic mechanisms of locomotion driven by surface chemical activity or solubilization. Crowdy [12] found analytical solutions for a two-dimensional phoretic Janus swimmer, including the situation where it swims near a flat no-slip wall; the swimmer was special in that it expelled and adsorbed a diffusive chemical species at its two faces in such a way that its effective far-field species concentration was dipolar, thereby circumventing mathematical obstructions associated with a purely diffusive source. At the same time, at zero Reynolds number, the swimmer motion was force-free, thereby also avoiding mathematical problems associated with the Stokes paradox. Sondak *et al.* [13] have studied the more general problem of phoretic motion of a two-dimensional Janus particle driven by the two-dimensional diffusion into the fluid surrounding the particle of a reactant entering via the active face. The interest there was in the consequences of the fact that a diffusive source term in two dimensions is divergent in the far field. With similar concerns in mind, Yariv and Crowdy [14] used an asymptotic analysis to examine the regularizing effect of species advection in the bulk (small Péclet number effects) on an isolated phoretic swimmer of this kind in the fast reaction limit. On the subject of isotropic particles, Hu *et al.* [15] showed that a rigid two-dimensional phoretic particle in an isotropic fluid can swim in circles at a critical value of the solute emission rate. Li [16] has used a weakly nonlinear analysis together with direct numerical simulations to study the effect of reaction rate on the dynamics of an active two-dimensional droplet swimming in a solution containing surfactants. Zhu and Zhu [17] were interested in the effect of particle shape on the dynamics and found that elliptical phoretic disks emitting solute uniformly can exhibit circular trajectories while simultaneously rotating.

Chemical reactions are not the only source of actuation: the speed of locomotion of an isolated two-dimensional Janus swimmer on which some stress distribution is imposed on its active face, with the other face being no-slip, has also been found analytically [18]. In that theoretical study, the physical origin of this actuating stress distribution was not discussed. One physical mechanism of much recent interest that produces such driving stresses for locomotion is the strategic release and subsequent spreading and diffusion of surfactants, either soluble or insoluble, to provoke a surface tension gradient and a concomitant surface Marangoni stress. This phenomenon is familiar in both natural biological [19] and synthetic situations [2–4]. Recent studies of "Marangoni surfers" [20,21] exploit stresses associated with surface gradients in both temperature and surfactant concentration to generate motion on free surfaces. An important theoretical study of viscous Marangoni propulsion caused purely by diffusion, rather than surface advection, of insoluble surfactant is by Lauga and Davis [22]. They considered a single thin circular disk floating on a semi-infinite layer of viscous fluid and self-actuated by the setting up of a prescribed surfactant distribution on a segment of its surface; there again, the physical mechanism whereby this surfactant distribution is set up is not discussed. The model assumes the surfactant is insoluble and that the Reynolds number, capillary number, and surface Péclet number are small so that locomotion of the disk is caused purely by the diffusion of the insoluble surfactant over the infinite free surface. Under the same modeling assumptions, Crowdy [23] found a formula for the speed of locomotion of a periodic array, or flotilla, of two-dimensional Marangoni boats, or floating strips, each driven by the release of surfactant onto the surface at their rear edge, which subsequently diffuses along the interfaces between the boats. An interesting feature of the latter study is a mathematical connection with solutions for shear flow

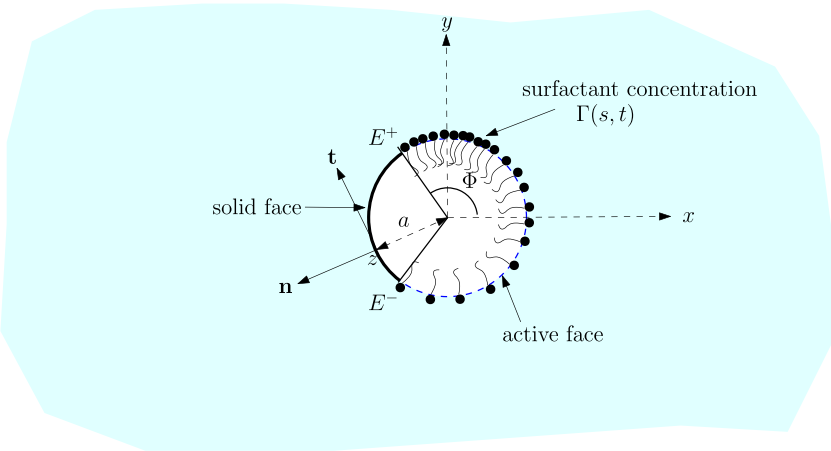

FIG. 1. Cotraveling frame of reference of a circular Janus swimmer of radius a in an unbounded fluid of viscosity μ with an active face comprising an insoluble-surfactant-bearing meniscus and an inert solid face. The two edges of the active face, at plane polar angles $\pm\Phi$, are denoted by $E^{\pm}$ as shown. The surfactant concentration at E^{+} is maintained at a higher level than that at E^{-}, causing surface diffusion of the insoluble surfactant between them.

over so-called superhydrophobic surfaces [24,25], something that will be discussed again later. In a similar vein, Nagai *et al.* [26] studied the surfactant dynamics and associated flow around a two-dimensional droplet with a point source of surfactant at its surface responsible for the Marangoni stress driving the motion. A pitchfork bifurcation from rectilinear motion to swimming in circles was observed as the droplet mobility increased.

The present article adds to this compendium of work on active two-dimensional Janus particles. A two-faced, two-dimensional, circular Janus swimmer is considered that is endowed with a "plastron," or active face made up of a free surface on which pure one-dimensional diffusion of an insoluble surfactant takes place, the other face being an inert, no-slip surface. A Marangoni stress is set up by maintaining a higher concentration of surfactant at one edge of the active face than at the other so that the insoluble surfactant diffuses along the surface between them. As in the prior studies of Lauga and Davis [22] and Crowdy [23], the regime considered is where the Reynolds, capillary, and surface Péclet numbers are all vanishingly small. Interestingly, the proposed surfactant-driven mechanism studied in this paper results in a nontrivial translational-rotational coupling in the isolated swimmer that leads to it swimming in a circle while spinning about its axis, a dynamical feature that has been observed in other settings [15–17,26] and is more usually associated with low-Reynolds-number swimming near solid boundaries [27]. A significant theoretical outcome of the present work is to show that this model problem can be solved analytically, allowing the multiphysics mechanism to be exemplified in explicit mathematical form.

II. AN ACTIVE JANUS SWIMMER

Consider a circular two-faced Janus particle, of radius a, centered at some instant at the origin in a Cartesian (x, y) plane as shown in Fig. 1. One of its faces, the "active face" or "plastron," comprises a free surface between an external viscous fluid of viscosity μ and an interior constant-pressure region, the other face is assumed to be an inert solid surface. The plastron is chosen to have a circular shape consistent with a Young-Laplace normal stress balance that would pertain in the high surface tension (small capillary number) limit, with the appropriate pressure difference maintained between the contained gas and a hydrostatic ambient fluid. In analogy with a superhydrophobic surface [25], the active face might be a circular-arc meniscus spanning the two sides of a "groove"

or notch made in an otherwise solid circular cylinder, trapping air in this groove in the so-called Cassie state. This notion of a "superhydrophobic cylinder" has recently been considered in other contexts [28–30].

If θ denotes the usual plane polar coordinate angle, then the active face is assumed, without loss of generality, to occupy the boundary portion

$$\theta \in (-\Phi, \Phi), \tag{1}$$

for some $0 \leqslant \Phi < \pi$. The active face is taken to be loaded with insoluble surfactant with average surfactant concentration Γ_0. If s is the arclength around the swimmer boundary in a cotraveling frame of reference, measured from the surface point $(a, 0)$ on the positive x axis, where $s = 0$, its surface tension $\sigma(s, t)$ is taken to depend on the surfactant concentration $\Gamma(s, t)$ according to the linear equation of state

$$\sigma(s, t) = \sigma_c - \beta\Gamma(s, t), \tag{2}$$

where σ_c is the surface tension of a clean face and $\beta = RT > 0$ where R is the gas constant and T the temperature, assumed here to be constant. Suppose that an insoluble surfactant is supplied/removed from the active face by imposing that the surfactant concentration at the edge E^+ at $s = -a\Phi$ shown in Fig. 1, is

$$\Gamma(-a\Phi, t) = \Gamma_0 + \Delta\Gamma/2, \tag{3}$$

where $\Delta\Gamma$ is externally imposed and taken here to be independent of Φ (although this restriction is easily generalized) with the surfactant concentration at the edge E^- at $s = a\Phi$ also labeled in Fig. 1, is set to be

$$\Gamma(a\Phi, t) = \Gamma_0 - \Delta\Gamma/2, \tag{4}$$

with the proviso that this is always non-negative. In this idealized theoretical model, the physical mechanism whereby this disparity in surfactant concentration across the active face is set up will not be discussed, however, provided that $0 < \Delta\Gamma \leqslant 2\Gamma_0$, as will be assumed, the surface tension at E^- will be greater than at E^+ causing fluid to be dragged clockwise around the plastron resulting in an expected anticlockwise rotation of the particle with some angular velocity $\Omega > 0$ to be determined. It is natural to impose a no-slip condition on the inert solid face of the swimmer. If the swimmer is to be free of any net external force and torque, it will generally move with some velocity (U_c, V_c) that must also be determined. For the analysis to follow, the frame of reference shown in Fig. 1 is taken to be a cotraveling frame of reference in which the particle is not displacing but may be rotating.

In this frame of reference, and assuming negligible inertia in the fluid, the velocity $\mathbf{u} = (u, v)$ of the fluid outside the particle satisfies the Stokes equations

$$\mu\nabla^2\mathbf{u} = \nabla p, \quad \nabla.\mathbf{u} = 0, \tag{5}$$

where p is the fluid pressure. The far-field condition is that

$$\mathbf{u} \to -(U_c, V_c), \quad \text{as } |\mathbf{x}| \to \infty. \tag{6}$$

On the inert solid face, the no-slip condition requires, adopting the usual summation convention, that

$$u_i t_i = -a\Omega, \quad u_i n_i = 0, \tag{7}$$

where, as shown in Fig. 1, t_i and n_i denote the components of the clockwise unit tangent vector $\mathbf{t}$ and fluid-inward normal vector $\mathbf{n}$, respectively, while on the active face, the condition is

$$t_i\sigma_{ij}n_j = -\frac{\partial\sigma}{\partial s}, \tag{8}$$

where

$$\sigma_{ij} = -p\delta_{ij} + 2\mu e_{ij}, \quad e_{ij} = \frac{1}{2}\left(\frac{\partial u_i}{\partial x_j} + \frac{\partial u_j}{\partial x_i}\right), \tag{9}$$

is the usual fluid stress tensor. Condition (8) says that the Marangoni stress caused by the surface tension gradient must be balanced locally by the tangential viscous stresses.

The challenge is to determine (U_c, V_c) and the angular velocity Ω of the Janus swimmer as it moves in response to the Marangoni stress set up on its active face. The full evolution equation for the surfactant concentration $\Gamma(s,t)$ on the active face of the Janus swimmer in the cotraveling frame is [31]

$$\frac{\partial \Gamma(s,t)}{\partial t} + \frac{\partial(\Gamma(s,t)U(s,t))}{\partial s} = D_s \frac{\partial^2 \Gamma(s,t)}{\partial s^2}, \tag{10}$$

where D_s is the surface diffusion coefficient and $U(s,t)$ denotes the slip velocity in the tangential direction around the surface. In general, this is a challenging nonlinear multiphysics problem since, even under the assumption of a quasisteady Stokes flow, (10) nonlinearly couples the interfacial surfactant evolution to the fluid flow. However, in line with previous work [22,23], the quantities (U_c, V_c) and Ω will now be determined explicitly in the limit where surface diffusion dominates surface advection of the surfactant on the active face, a situation that affords simplifications that render the problem mathematically tractable.

III. COMPLEX VARIABLE FORMULATION

With the introduction of the complex variable $z = x + \mathrm{i}y$ in the cotraveling frame, the particle boundary corresponds to $|z| = a$ and the fluid of viscosity μ occupies $|z| > a$. On taking the curl of (5), it is well known [23,32] that a two-dimensional Stokes flow is describable by a biharmonic streamfunction $\psi(z,\bar{z})$ associated with flow $\mathbf{u} = (u, v)$ given by

$$\psi(z,\bar{z}) = \mathrm{Im}[\bar{z}f(z) + g(z)], \quad (u, v) = \left(\frac{\partial \psi}{\partial y}, -\frac{\partial \psi}{\partial x}\right), \tag{11}$$

where $f(z)$ and $g(z)$ are two (Goursat) functions of $z = x + \mathrm{i}y$ analytic for $|z| > a$ but with possible singularities at infinity. Although the particle is moving, the quasisteady Stokes flow must be found at each instant, so the parametric dependence of all variables on time t is now suppressed and only reinstated when the particle dynamics is considered in Sec. VI.

It can be shown that the fluid pressure p, the vorticity $\omega = -\nabla^2\psi$, and the fluid rate-of-strain tensor e_{ij} are related to $f(z)$ and $g(z)$ through

$$4f'(z) = \frac{p}{\mu} - \mathrm{i}\omega, \quad u - \mathrm{i}v = -\overline{f(z)} + \bar{z}f'(z) + g'(z), \quad e_{11} + \mathrm{i}e_{12} = z\overline{f''(z)} + \overline{g''(z)}, \tag{12}$$

where the prime notation denotes differentiation with respect to z. The complex form of the fluid stress on the boundary, i.e., $-pn_i + 2\mu e_{ij}n_j$, is

$$-2\mu \mathrm{i}\frac{dH}{ds}, \quad H(z,\bar{z}) = f(z) + z\overline{f'(z)} + \overline{g'(z)}, \tag{13}$$

where the arclength s along the circular boundary increases in a tangential direction. A fuller derivation of this complex variable formulation of two-dimensional quasisteady Stokes flow can be found in an Appendix of Crowdy [23]. A useful observation, which follows from the chain rule given that $z = ae^{-\mathrm{i}s/a}$, is

$$\frac{\partial}{\partial s} = -\frac{\mathrm{i}z}{a}\frac{\partial}{\partial z}. \tag{14}$$

The complex version of the unit tangent and normal vectors is therefore

$$-\frac{\mathrm{i}z}{a}, \quad \frac{z}{a}, \tag{15}$$

respectively.

IV. A MIXED BOUNDARY VALUE PROBLEM

The boundary conditions on the two faces of the Janus particle must now be reformulated as conditions on the Goursat functions. The function $f(z)$ must be single valued and analytic in $|z| > a$ except for a simple pole at infinity, where

$$f(z) \to \frac{p_\infty}{4\mu} z + f_\infty + \mathcal{O}(1/z), \tag{16}$$

where the real constant p_∞ denotes the fluid pressure at infinity and $f_\infty \in \mathbb{C}$ is a complex constant that will be related shortly to the cylinder velocity (U_c, V_c). The single-valuedness of $f(z)$ ensures that there is no net force on the cylinder, as can be seen by integration of the boundary fluid stress (13) around the cylinder boundary while bearing in mind that $f(z)$ and $g'(z)$ must be such that $u - \mathrm{i}v$ as given by (12) is necessarily single-valued in the fluid region. Note also that the far-field form (16) ensures that there is no vorticity as $|z| \to \infty$.

Let

$$g(z) = -\frac{a^2 f(z)}{z}. \tag{17}$$

This ensures that the streamline condition on the surface of the Janus particle is satisfied; this is readily checked on the substitution of (17) into (11). At the same time, the choice (17) ensures that the total torque on the swimmer is zero since an external torque would require a logarithmic singularity of $g(z)$ at infinity. The complex conjugate velocity field is then given by

$$u - \mathrm{i}v = -\overline{f(z)} + \overline{z} f'(z) + g'(z) = -\overline{f(z)} + \overline{z} f'(z) - \frac{a^2 f'(z)}{z} + \frac{a^2 f(z)}{z^2}. \tag{18}$$

On the use of (6), (12), and (18), it follows that

$$f_\infty = U_c + \mathrm{i}V_c. \tag{19}$$

On the swimmer boundary, $|z| = a$ where $\overline{z} = a^2/z$, (18) reduces to

$$u - \mathrm{i}v = -\overline{f(z)} + \frac{a^2 f(z)}{z^2}. \tag{20}$$

If $U(s) = \mathbf{u}.\mathbf{t}$ is used to denote the tangential slip velocity, then

$$U(s) = \mathrm{Re}\left[(u - \mathrm{i}v)\left(-\frac{\mathrm{i}z}{a}\right)\right] = \mathrm{Re}\left[-\mathrm{i}\left(\frac{af(z)}{z} - \overline{\left(\frac{af(z)}{z}\right)}\right)\right] = a\mathrm{Im}\left[\frac{2f(z)}{z}\right], \tag{21}$$

where (15) has been used, as well as the fact that if two vectors $\mathbf{a} = (a_x, a_y)^T$ and $\mathbf{b} = (b_x, b_y)^T$ have complex counterparts $a = a_x + \mathrm{i}a_y$ and $b = b_x + \mathrm{i}b_y$, respectively, then the dot product $\mathbf{a}.\mathbf{b} = \mathrm{Re}[\overline{a}b]$ where $\overline{a}$ is the complex conjugate of a. On the solid portions of the particle, it follows from (7) that

$$U(s) = -a\Omega, \tag{22}$$

where Ω is the angular velocity of the particle in the anticlockwise direction; the minus sign appears because $U(s)$ is the slip velocity in the clockwise tangential direction. Hence, on the solid portions

of the particle boundary, (21) implies that

$$a\mathrm{Im}[h(z)] = -a\Omega, \tag{23}$$

where

$$h(z) \equiv \frac{2f(z)}{z}, \tag{24}$$

which is analytic and single-valued in $|z| > 1$, including at infinity where, as $|z| \to \infty$,

$$h(z) \sim \frac{p_\infty}{2\mu} + \frac{2(U_c + \mathrm{i}V_c)}{z} + \mathcal{O}(1/z^2), \tag{25}$$

where (16) has been used.

On the active face of the Janus swimmer, the Marangoni stress condition (8) implies

$$\mathrm{Re}\left[\left(\frac{\mathrm{i}\bar{z}}{a}\right)\left(-2\mu\mathrm{i}\frac{dH}{ds}\right)\right] = \beta\frac{\partial\Gamma}{\partial s}, \tag{26}$$

where the equation of state (2) has been used. Equivalently, since $\bar{z} = a^2/z$ on the active face, this condition is

$$\mathrm{Re}\left[\frac{2\mu a}{z}\frac{dH}{ds}\right] = \mathrm{Re}\left[\frac{2\mu a}{z}\left(-\frac{\mathrm{i}z}{a}\right)\frac{dH}{dz}\right] = \beta\frac{\partial\Gamma}{\partial s}. \quad \text{or} \quad \mathrm{Im}\left[\frac{dH}{dz}\right] = \frac{\beta}{2\mu}\frac{\partial\Gamma}{\partial s}, \tag{27}$$

where (14) has been used. Since, from (17),

$$H(z,\bar{z}) = f(z) + z\overline{f'(z)} - \overline{\left(\frac{a^2 f'(z)}{z}\right)} + \frac{a^2\overline{f(z)}}{\bar{z}^2}, \tag{28}$$

then, on $|z| = a$,

$$\frac{H(z,\bar{z})}{z} = \mathrm{Re}\left[\frac{2f(z)}{z}\right]. \tag{29}$$

It follows that

$$H(z,\bar{z}) = z\mathrm{Re}[h(z)], \tag{30}$$

implying, on differentiation with respect to z, that

$$\frac{dH}{dz} = \mathrm{Re}[h(z)] + z\frac{d}{dz}\mathrm{Re}[h(z)] = \mathrm{Re}[h(z)] + \mathrm{i}a\frac{d}{ds}\mathrm{Re}[h(z)], \tag{31}$$

where (14) has been used again. On the use of this relation, condition (27) becomes

$$\mathrm{Im}\left[\frac{dH}{dz}\right] = \mathrm{Im}\left[\mathrm{i}a\frac{d}{ds}\mathrm{Re}[h(z)]\right] = a\frac{d}{ds}\mathrm{Re}[h(z)] = \frac{\beta}{2\mu}\frac{\partial\Gamma}{\partial s}. \tag{32}$$

This can be integrated with respect to s to give

$$a\mathrm{Re}[h(z)] = \frac{\beta}{2\mu}\Gamma, \tag{33}$$

where a constant of integration has been set equal to zero without loss of generality, since it corresponds to setting a baseline fluid pressure that does not affect the flow.

The surfactant evolution equation (10) can be written in nondimensional form as

$$\frac{\partial\Gamma(s,t)}{\partial t} + \frac{\partial(\Gamma(s,t)U(s,t))}{\partial s} = \frac{1}{Pe_s}\frac{\partial^2\Gamma(s,t)}{\partial s^2}, \tag{34}$$

where the same symbols are now used to denote nondimensional counterparts to all quantities, and the surface Péclet number is defined as

$$Pe_s = \frac{U_0 a}{D_s}. \tag{35}$$

Lengths have been nondimensionalized with respect to a, velocity with a natural velocity scale U_0 to be selected shortly, and time with a/U_0. In the diffusion-dominated limit $Pe_s \to 0$ of interest here, (34) reduces to

$$\frac{\partial^2 \Gamma}{\partial s^2} = 0, \quad \text{or} \quad \Gamma(s) = A + Bs, \quad A, B \text{ constants}, \tag{36}$$

which linearizes the problem since the coupling with the tangential slip velocity is now lost, and the distribution of surfactant is also now quasisteady. Since the swimmer speed is expected to depend on the difference $\Delta\Gamma$ between surfactant concentrations at $E^{\pm}$, it is natural to choose the velocity scale

$$U_0 = \frac{\beta \Delta\Gamma}{2\mu}. \tag{37}$$

Using $\Delta\Gamma$ to nondimensionalize the surfactant concentration, the challenge now is to find a nondimensional function $h(z)$, analytic and single-valued in $|z| > 1$, satisfying the mixed boundary conditions

$$\begin{aligned} &\text{Re}[h(z)] = \Gamma(s), \quad &&\text{on the active face,} \\ &\text{Im}[h(z)] = -\Omega, \quad &&\text{on the solid face,} \end{aligned} \tag{38}$$

with

$$\text{Im}[h(z)] \to 0, \quad \text{as} \|z| \to \infty, \tag{39}$$

in order to be consistent with (25). Moreover, it follows from (36), on the use of the surface boundary conditions (3) and (4), that on the active face,

$$\Gamma(s) = \overline{\Gamma_0} - Js, \quad J = \frac{1}{2\Phi}, \tag{40}$$

where $\overline{\Gamma_0}$ is the nondimensionalized average surfactant level, i.e., $\Gamma_0 = (\Delta\Gamma)\overline{\Gamma_0}$. The parameter J can be understood as the non-dimensional surfactant concentration gradient maintained across the active face. Note that $J \to \infty$ as $\Phi \to 0$ but, in this same limit, the active face disappears, so this limit is expected to be regular. With the surfactant concentration found, it only remains to solve for the associated Stokes flow or, equivalently, to find $h(z)$. In view of (40), the boundary conditions (38) for $h(z)$ become

$$\begin{aligned} &\text{Re}[h(z)] = \overline{\Gamma_0} - Js, \quad &&\text{on the active face of } |z| = 1, \\ &\text{Im}[h(z)] = -\Omega, \quad &&\text{on the solid face of } |z| = 1. \end{aligned} \tag{41}$$

This is a mixed boundary value problem for the function $h(z)$, analytic and single-valued in $|z| > 1$, having the special feature that the boundary data is determined except for the value of the unknown angular velocity Ω. Note also that the nature of the mixed boundary conditions (41), corresponding physically to a transition, from a slip condition to a specified shear stress condition, implies that square root singularities of $h(z)$ are expected at the edges $E^{\pm}$ of the active face [24,25].

V. SOLUTION USING CONFORMAL SLIT MAPPINGS

It will now be shown that this mixed boundary value problem for $h(z)$ can be solved analytically using conformal slit mappings [25,33,34], a natural way to solve such mixed boundary value problems since the square-root singularities at the edges $E^{\pm}$ can be accounted for intrinsically in such a parametric description.

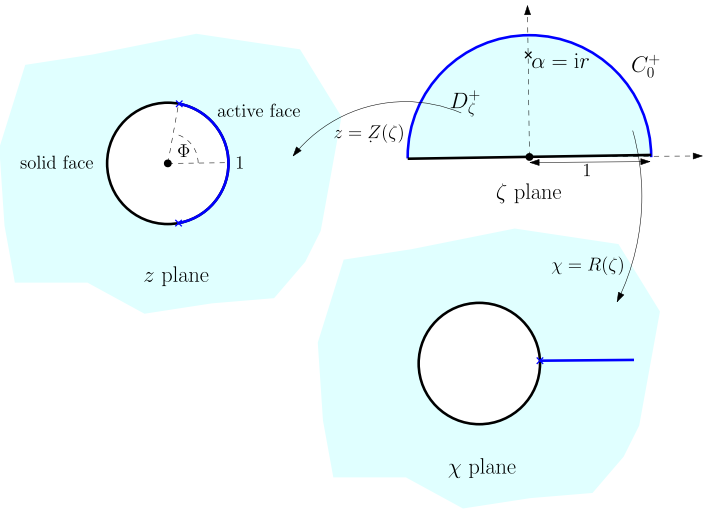

FIG. 2. Conformal slit mappings, $Z(\zeta)$ and $\mathcal{R}(\zeta)$, from an upper-half unit disk $\{D_\zeta^+ : |\zeta| < 1, \mathrm{Im}[\zeta] \geqslant 0\}$ to an unbounded circular slit domain (in a complex z plane) and an unbounded radial slit domain (in a complex χ plane). Corresponding images under the respective maps are color coded. The point $\zeta = \alpha$ is the preimage of the origin in both cases.

The first step is to introduce a conformal mapping from the upper-half unit ζ disk, denoted by $D_\zeta^+ = \{\zeta \,||\zeta| < 1, \mathrm{Im}[\zeta] > 0\}$ to the fluid region; Fig. 2 shows a schematic. It is given by

$$z = Z(\zeta) \equiv -\frac{(\zeta - \overline{\alpha})(\zeta - 1/\overline{\alpha})}{(\zeta - \alpha)(\zeta - 1/\alpha)}, \quad \alpha = \mathrm{i}r, \tag{42}$$

for some $0 \leqslant r < 1$. This mapping is an example of an important class known as unbounded circular-slit mappings [34]. Using this definition, it is easy to check that both the upper-half unit semicircle, denoted by C_0^+, is transplanted to a portion of the circle $|z| = 1$ while the real diameter $-1 < \zeta < 1$ is transplanted to the remainder of this circle. It is also easily verified that

$$Z(0) = -1, \quad Z(1) = \left(\frac{1+\alpha}{1-\alpha}\right)^2, \quad Z(\mathrm{i}) = 1. \tag{43}$$

The semicircle C_0^+ can be identified with the preimage of the meniscus, and the real diameter $-1 < \zeta < 1$ is the preimage of the no-slip portion of the swimmer. The center of the active face at $z = 1$ is $\zeta = \mathrm{i}$. The preimage of E^+ is $\zeta = 1$ meaning that

$$Z(1) = \left(\frac{1+\alpha}{1-\alpha}\right)^2 = \left(\frac{1+\mathrm{i}r}{1-\mathrm{i}r}\right)^2 = e^{\mathrm{i}\Phi}, \quad \text{or} \quad \frac{1+\mathrm{i}r}{1-\mathrm{i}r} = e^{\mathrm{i}\Phi/2}. \tag{44}$$

Simple manipulation of this relation and use of familiar trigonometric identities yield

$$r = \tan(\Phi/4). \tag{45}$$

Given explicit knowledge of the conformal mapping $Z(\zeta)$, the composed function

$$H(\zeta) \equiv h(Z(\zeta)), \tag{46}$$

can be introduced which, by virtue of the respective analyticity properties of $h(z)$ and $Z(\zeta)$, is analytic in D_ζ^+ and must tend to a real constant as $\zeta \to \alpha$ in order that there is no vorticity in the far field, as can be seen from the expression for $f'(z)$ in (12). In view of (41), on the boundary of D_ζ^+

the function $H(\zeta)$ must satisfy

$$\begin{aligned} &\mathrm{Re}[H(\zeta)] = \overline{\Gamma_0} - Js, \quad \text{on } C_0^+, \\ &\mathrm{Im}[H(\zeta)] = -\Omega, \qquad \text{on } -1 < \mathrm{Re}[\zeta] < 1, \quad \mathrm{Im}[\zeta] = 0. \end{aligned} \tag{47}$$

It is useful now to write down another conformal slip mapping to a complex χ plane, called a radial-slit mapping [34], having a similar form to (42) but defined by

$$\chi = \mathcal{R}(\zeta) \equiv -\frac{(\zeta - \overline{\alpha})(\zeta - 1/\alpha)}{(\zeta - \alpha)(\zeta - 1/\overline{\alpha})}. \tag{48}$$

Notice that, while the first term in the numerators and denominators of (42) and (48) are the same, the second terms have been swapped. As shown in Fig. 2, the image of D_ζ^+ under this mapping is the exterior of the circular disk $|\chi| > 1$ with C_0^+ being transplanted to a radial slit on the positive real χ axis and the real diameter $-1 < \mathrm{Re}[\zeta] < 1$ being transplanted to the entire circle $|\chi| = 1$. These properties can be checked directly using formula (48): it is easy to check, for example, that the image of C_0^+ is purely real and positive, and that

$$\mathcal{R}(1) = 1, \quad \mathcal{R}(-1) = 1. \tag{49}$$

It can now be argued, based on the geometry of these mappings, that the expression

$$H(\zeta) = \overline{\Gamma_0} - \mathrm{i}\Omega - \mathrm{i}J(\log Z(\zeta) - \log \mathcal{R}(\zeta)), \tag{50}$$

involving both the bounded circular-slit mapping $Z(\zeta)$ and the radial-slit mapping $\mathcal{R}(\zeta)$, is the required solution for $H(\zeta)$ provided that Ω is chosen appropriately. First, note that both mappings $Z(\zeta)$ and $\mathcal{R}(\zeta)$ have simple zeros at $\zeta = \alpha$ in D_ζ^+, but the resulting logarithmic singularities in (50) cancel out, meaning that the function $H(\zeta)$ in (50) is analytic in D_ζ^+, as required. On C_0^+, which corresponds to the active face of the Janus swimmer, $z = Z(\zeta) = e^{-\mathrm{i}s}$ so that $\log Z(\zeta) = -\mathrm{i}s$ and $\arg[\mathcal{R}(\zeta)] = 0$, therefore, it can be verified that the first of the boundary conditions in (47) is satisfied. And, since the real diameter $-1 < \mathrm{Re}[\zeta] < 1$, corresponding to the solid face of the Janus swimmer, is transplanted to a unit circle (in the respective target plane) by both slit mappings $Z(\zeta)$ and $\mathcal{R}(\zeta)$ then $\mathrm{Im}[H(\zeta)] = -\Omega$ on this real diameter, thus (50) also satisfies the second of the boundary conditions in (47). Only one further requirement remains: to arrange that $H(\alpha)$ is a purely real constant to satisfy (39). On the use of (42) and (48) in (50), it follows that

$$H(\zeta) = \overline{\Gamma_0} - \mathrm{i}\Omega - 2\mathrm{i}J \log\left(\frac{1/\alpha + \zeta}{1/\alpha - \zeta}\right). \tag{51}$$

It can be checked that this expression satisfies $\mathrm{Re}[H(\mathrm{i})] = \overline{\Gamma_0}$, which is consistent with (47) when $s = 0$ at the center of the active face. Hence, condition (39) requires

$$\mathrm{Im}[H(\alpha)] = -\Omega - 2J \log\left|\frac{1/\alpha + \alpha}{1/\alpha - \alpha}\right| = 0, \tag{52}$$

which, on rearrangement and use of $\alpha = \mathrm{i}r$, gives the angular velocity of the swimmer

$$\Omega = -2J \log\left(\frac{1 - r^2}{1 + r^2}\right) = 2J \log \sec(\Phi/2), \tag{53}$$

after use of (45) and trigonometric identities. The angular velocity Ω of the Janus swimmer has therefore been determined, as has the complex potential $h(z)$ since it is given in (51) as an explicit function of ζ with Ω given by (53). The entire flow field has therefore been determined. Even though $J \to \infty$ as $\Phi \to 0$, the angular velocity $\Omega \to 0$ in this limit of the active face disappearing. Also note that $\Omega > 0$ when $J > 0$ corresponding to anticlockwise particle rotation, as anticipated earlier. As the active face covers more of the swimmer surface, the angular velocity increases, eventually becoming unbounded as $\Phi \to \pi$. This is to be expected because, as the size of the inert no-slip face decreases, so too will its resistance to the flow set up by the Marangoni stress.

The speed (U_c, V_c) of the swimmer follows from the asymptotics of $H(\zeta)$ near $\zeta = \alpha$ corresponding to the far-field asymptotics of $h(z)$. Near $\zeta = \alpha$ a Taylor expansion of (51) implies that

$$H(\zeta) = \overline{\Gamma_0} - \mathrm{i}\Omega - 2\mathrm{i}J \log\left(\frac{1/\overline{\alpha} - \alpha}{1/\alpha - \alpha}\right) + (\zeta - \alpha)\left[-2\mathrm{i}J\left(\frac{1}{\alpha - 1/\overline{\alpha}} - \frac{1}{\alpha - 1/\alpha}\right)\right] + \ldots$$
$$= \overline{\Gamma_0} + \frac{4AJr}{1 - r^4}\frac{1}{z} + \ldots, \tag{54}$$

where (53) has been used together with the fact that

$$z = Z(\zeta) \to \frac{A}{\zeta - \alpha} + \ldots, \tag{55}$$

as $\zeta \to \alpha$ where, from a local analysis of (42) as $\zeta \to \alpha$,

$$A = \frac{2\mathrm{i}r(1 - r^2)}{(1 + r^2)}. \tag{56}$$

On comparison of (25) with (54), it follows that

$$2(U_c + \mathrm{i}V_c) = \frac{8\mathrm{i}Jr^2}{(1 + r^2)^2}, \tag{57}$$

or

$$U_c = 0, \quad V_c = J\left(\frac{2r}{1 + r^2}\right)^2 = J\sin^2(\Phi/2), \tag{58}$$

where (45) has been used. Therefore, the swimmer does not displace in the direction of its axis of symmetry, a result that can be anticipated *a priori* using reversibility arguments for Stokes flow and the fact that the induced Marangoni stress on the active face is constant in the zero surface Péclet number regime. The swimmer does, however, move perpendicular to its axis of symmetry. Given that the particle is rotating with nonzero angular velocity Ω given in (53), it follows that there is a nontrivial translational-rotational coupling associated with the motion of this Janus swimmer actuated by pure diffusion of the insoluble surfactant. Notice again that although $J \to \infty$ as $\Phi \to 0$, the speed in this perpendicular direction $V_c \to 0$ in this limit of the active face disappearing. Of interest is that $V_c \to J$ as $\Phi \to \pi$, so the displacement speed tends to a finite value even as the angular velocity $\Omega \to \infty$ in this singular limit.

While the above analysis completes a parametric representation of the solution in terms of ζ, it turns out to be possible to eliminate the variable ζ between (42) and formula (51) to find the explicit result

$$h(z) = \overline{\Gamma_0} - \mathrm{i}\Omega + 2J\left[\cos^{-1}\left(\frac{\cos\kappa(z)}{\cos(\Phi/2)}\right) - \kappa(z)\right], \quad \kappa(z) = \frac{\mathrm{i}}{2}\log z. \tag{59}$$

Further details of the derivation of (59) are given in Appendix. A local analysis of (59) near the edges $E^{\pm}$ of the active face, not included here, reveals the aforementioned square root singularities of $h(z)$ expected at those points. With $h(z)$ thus determined in (59), a formula for $f(z)$ follows from (24), $g(z)$ is given in (17), and the flow streamfunction

$$\psi(z, \overline{z}) = \tfrac{1}{2}\mathrm{Im}[(z\overline{z} - 1)h(z)], \tag{60}$$

defined in (11) is now known as an explicit function of z.

Figure 3 shows four instantaneous streamline distributions around Janus swimmers with active faces having half-opening-angles $\Phi = \pi/6, \pi/3, \pi/2$ and $3\pi/4$. These can be readily produced as contour plots using the streamfunction (60). In practice, however, it is more convenient to plot these contours using the parametric form of the solution with z and $h(z)$ given, as functions of the parametric variable ζ, by (42) and (51), respectively, one reason being that the half-disk ζ domain

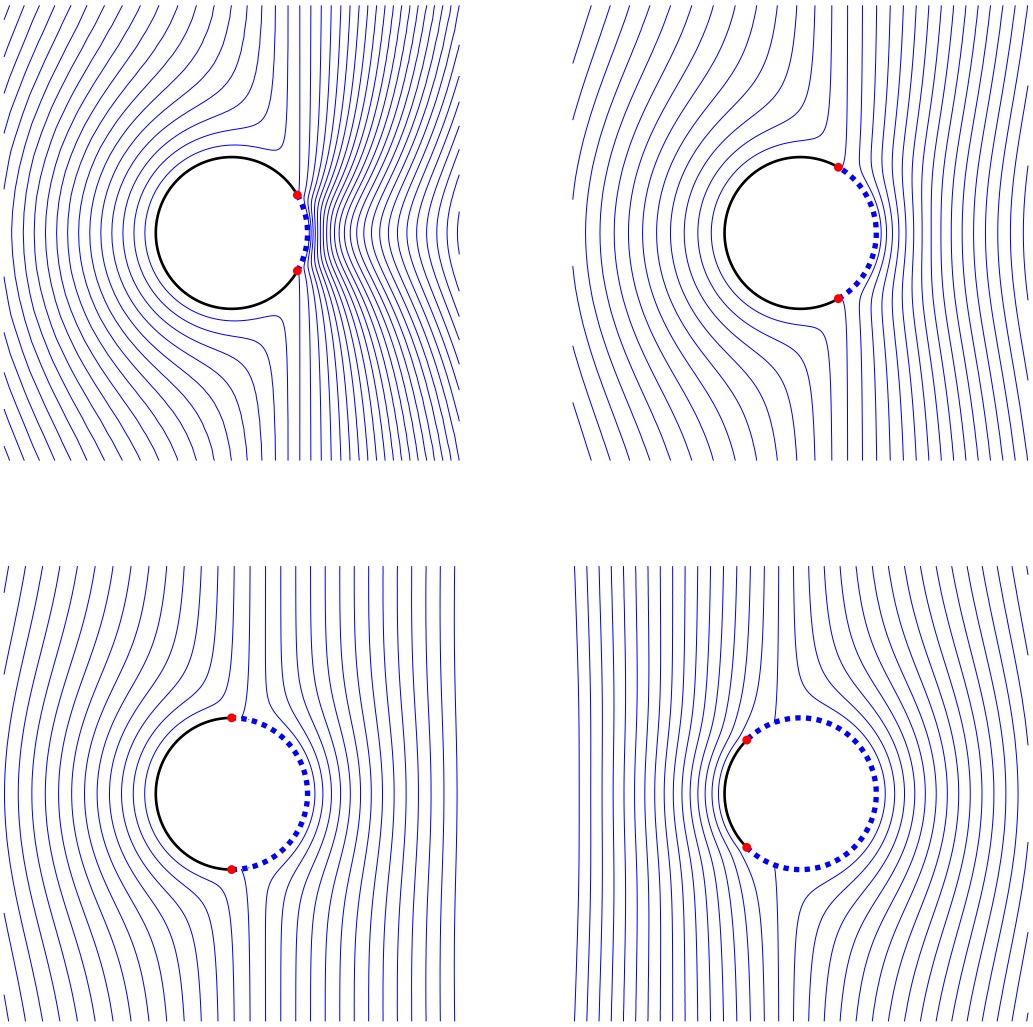

FIG. 3. Instantaneous streamlines around Janus swimmers with $\Phi = \pi/6, \pi/3, \pi/2$, and $3\pi/4$. In this cotraveling frame, two stagnation points, at reflectionally symmetric points relative to the axis of symmetry of the swimmer, move closer to the edges $E^{\pm}$ (shown red) as Φ decreases. Separatrix streamlines emanating from those stagnation points are shown.

is finite and therefore easier to mesh. It is observed that the active face has two stagnation points, at reflectionally symmetric points relative to the real axis, that move closer to the edges $E^{\pm}$ as Φ decreases.

VI. DYNAMICS OF THE JANUS SWIMMER

With the quasisteady low-Reynolds-number flow field at each instant now determined, focus shifts to the dynamics of the swimming particle. Let the position of a time-evolving Janus swimmer be $(X_c(t), Y_c(t))$ and let $\Theta(t)$ be the angle made by its axis of symmetry with the positive real axis. If $Z_c(t) = X_c(t) + \mathrm{i}Y_c(t)$ the ordinary differential equations governing the swimmer motion can be

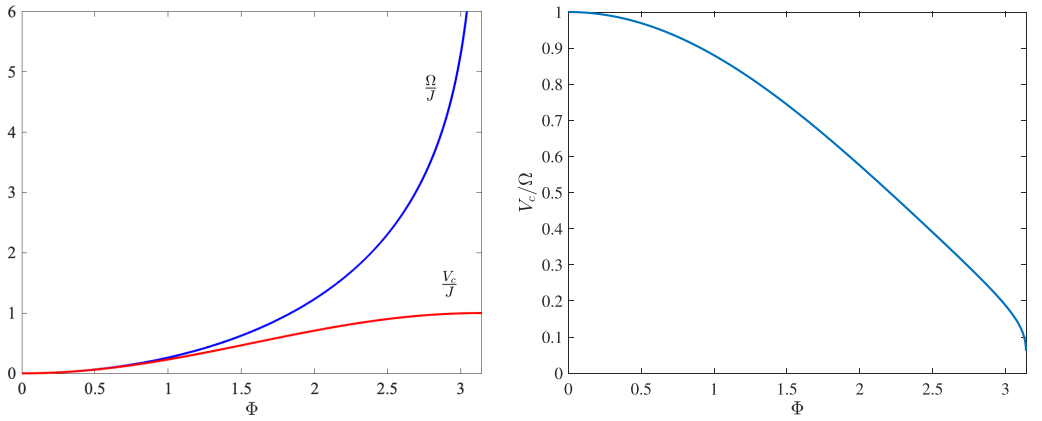

FIG. 4. Graphs of V_c/J, Ω/J (left) and trajectory radius $R = V_c/\Omega$ (right) as a function of half-angle Φ of the active face of the Janus swimmer.

shown to be given by

$$\frac{dZ_c}{dt} = \mathrm{i}V_c e^{\mathrm{i}\Theta}, \quad \frac{d\Theta}{dt} = \Omega, \tag{61}$$

where V_c and Ω have been determined as functions of J and the swimmer geometry Φ, respectively, in the previous section. If initial conditions are chosen so that $\Theta(0) = 0$ and $Z_c(0) = 0$ then

$$\Theta(t) = \Omega t, \tag{62}$$

and

$$\frac{dZ_c}{dt} = \mathrm{i}V_c e^{\mathrm{i}\Omega t}, \quad Z_c(t) = \frac{V_c}{\Omega}(e^{\mathrm{i}\Omega t} - 1). \tag{63}$$

On introducing

$$R = \frac{V_c}{\Omega} = \frac{\sin^2(\Phi/2)}{2\log\sec(\Phi/2)}, \tag{64}$$

then

$$\frac{X_c(t)}{R} = \cos\Omega t - 1, \quad \frac{Y_c(t)}{R} = \sin\Omega t, \tag{65}$$

implying that the trajectory of the particle center lies on

$$(X_c + R)^2 + Y_c^2 = R^2, \tag{66}$$

which is a circle of radius R centered at $(-R, 0)$. If $\Omega = 0$, corresponding to $\Phi = 0$, the particle lies on this circle but it is stationary at the origin, as expected, since the source of locomotion has been lost. For $\Phi \neq 0$, the particle rotates about its axis and simultaneously travels around the circular trajectory given by (66). Figure 4 shows graphs of V_c/J and Ω/J as a function of half-angle Φ of the active face. Also shown in Fig. 4 is the trajectory radius $R = V_c/\Omega$ as a function of Φ. This radius is independent of J and depends only on the particle geometry. One interesting feature of this graph is that the maximum displacement from its original center location that such a swimmer can achieve is bounded above by its diameter, although it is not possible to attain this upper bound. The smaller the active face, the larger the trajectory radius, although in the limit of the active face disappearing, the angular and translational velocities of the Janus particle both vanish, rendering the particle stationary. For a swimmer to increase the maximum displacement from its

initial location, the fraction of its surface area occupied by the active face should be reduced. It can attain its maximum displacement more quickly if the active face is larger, but at the price of reducing the maximum possible displacement. The swimmer problem is not well defined at the limiting value $\Phi = \pi$: as $\Phi \to \pi$ the swimmer rotates increasingly quickly, but the radius of its circular trajectory decreases, even as its velocity V_c along this path saturates to a finite value.

VII. SUMMARY AND DISCUSSION

An exact solution has been obtained for the Stokes flow around an active circular two-dimensional Janus swimmer driven by diffusion of insoluble surfactant from one edge of its active face to the other. The results allow for a translational-rotational coupling associated with this Marangoni-driven migration mechanism to be exhibited in an explicit mathematical fashion. While the Reynolds, capillary, and surface Péclet numbers have all been assumed to be vanishingly small, the fact that nontrivial analytical solutions are available in this leading-order model of a Marangoni-driven Janus swimmer is expected to be useful when adding in additional effects perturbatively. This might include weak inertial effects (small but nonzero Reynolds number), weak surface advection of the insoluble surfactant (small but nonzero surface Péclet number), or weak solubility of the surfactant to the bulk (small but nonzero Biot number). This work complements a previously derived exact solution [12] for the flow around a two-dimensional Janus particle driven by an imposed distribution of stress on its active face with the important difference that, here, the physical origin of the driving stress distribution has also been resolved: it is a Marangoni stress caused by surface diffusion of insoluble surfactant over the active face and its functional form cannot be chosen arbitrarily but follows from the governing equations to be (40), in nondimensional form.

Mathematically, the solution here can be understood as the radial analog of the author's solution for a flotilla, or periodic array, of Marangoni boats translating along an infinite free surface [23]. As mentioned earlier, the latter solution is closely related to the problem of simple shear over a periodic superhydrophobic surface [24,25]: on subtracting off from such a flow a simple Couette flow so as to cancel out the far-field shear, a constant shear stress then appears on the previously shear-free surface that can be interpreted differently as that induced by diffusion of an insoluble surfactant in the zero Péclet number limit. In the same way, the new solution for a viscous Marangoni Janus swimmer presented in this paper is closely related to a recently derived exact solution for a torque-driven superhydrophobic cylinder [30] having the same Janus-type geometry: on subtracting from that flow the flow due to a pure rotlet at the swimmer center and having the same torque, the particle becomes torque-free, its angular velocity changes, and a constant shear stress appears on the previously stress-free face that can similarly be viewed differently as the stress on the active face, or plastron, of a swimmer induced by diffusion of an insoluble surfactant in the zero Péclet number limit. Indeed, it should be emphasized that the results here could have been rederived by simply importing the previously derived solution for a torque-driven superhydrophobic cylinder with a single meniscus [30] and subtracting off a pure rotlet flow in this way. However, the single-meniscus solution for a torque-driven superhydrophobic cylinder was derived previously by the author [30] as a "single-meniscus limit" of a more complicated solution for a superhydrophobic cylinder with two unequal menisci and involving the use of a special transcendental function known as the prime function [34]. Since that transcendental function is not needed for the Janus swimmer considered here, it was thought more instructive to present a direct construction of the swimmer solution by a method that emulates, but both modifies and simplifies, that used for the two-meniscus torque-driven cylinder [30].

The swimmer considered here is a theoretical idealization, not least in being a two-dimensional entity. As just explained, its conceptualization originates in recent work on superhydrophobic surfaces, which are characterized by mixtures of no-slip and no-shear surfaces [24,25,28–30]. On a practical level, how such a swimmer with a free-surface plastron might be set up and a surfactant gradient across it maintained is not clear. Nevertheless, the analysis of the model is useful in being reflective of the minimal ingredients needed to set up an analogous translational-rotational coupling

in a more realistic anisotropic three-dimensional swimmer. No chemical reactions at the interface are needed, or indeed any form of interaction of the surface activity with the bulk (e.g., solubility, or adsorption/desorption to the ambient fluid). All that is needed is an anisotropic geometry, such as the two faces of the Janus swimmer studied here, together with some means of exerting a constant shear stress across one of those faces.

ACKNOWLEDGMENTS

This work is partly funded by EPSRC Grant No. EP/V062298/1.
The author declares no competing interests.

DATA AVAILABILITY

All graphs shown in the paper have been generated using explicit formulas included in the body of the paper. The data that support the findings of this article are not publicly available. The data are available from the author upon reasonable request.

APPENDIX: EXPLICIT SOLUTION FOR $h(z)$

It follows from the use of (42) and (48) in (50) that

$$H(\zeta) = \overline{\Gamma_0} - \mathrm{i}\Omega - 2\mathrm{i}J\mathcal{H}(\zeta), \tag{A1}$$

where

$$\mathcal{H}(\zeta) = \log\left(\frac{1/\alpha + \zeta}{1/\alpha - \zeta}\right). \tag{A2}$$

It follows that

$$\frac{1/\alpha + \zeta}{1/\alpha - \zeta} = e^{\mathcal{H}(\zeta)}, \tag{A3}$$

which can be rearranged to give

$$\zeta = \frac{1}{\alpha}\left(\frac{e^{\mathcal{H}(\zeta)} - 1}{e^{\mathcal{H}(\zeta)} + 1}\right). \tag{A4}$$

On taking a logarithm of (42),

$$\log z = \log\left(\frac{\zeta + \alpha}{\zeta - \alpha}\right) + \mathcal{H}(\zeta). \tag{A5}$$

Now, introduce

$$\kappa = \frac{\mathrm{i}}{2}\log z, \quad \log z = -2\mathrm{i}\kappa, \tag{A6}$$

so that (A5) becomes

$$-2\mathrm{i}\kappa - \mathcal{H}(\zeta) = \log\left(\frac{\zeta + \alpha}{\zeta - \alpha}\right). \tag{A7}$$

On exponentiation, it follows that

$$\frac{\zeta + \alpha}{\zeta - \alpha} = e^{-2\mathrm{i}\kappa - \mathcal{H}(\zeta)}, \tag{A8}$$

which can be rearranged to give

$$\zeta = \alpha\left(\frac{e^{-2i\kappa-\mathcal{H}(\zeta)}+1}{e^{-2i\kappa-\mathcal{H}(\zeta)}-1}\right). \tag{A9}$$

The two expressions for ζ in (A4) and (A9) can now be set equal to eliminate ζ and provide a relationship between z and $\mathcal{H}(\zeta)$:

$$\frac{1}{\alpha}\left(\frac{e^{\mathcal{H}(\zeta)}-1}{e^{\mathcal{H}(\zeta)}+1}\right) = \alpha\left(\frac{e^{-2i\kappa-\mathcal{H}(\zeta)}+1}{e^{-2i\kappa-\mathcal{H}(\zeta)}-1}\right). \tag{A10}$$

It follows that

$$\frac{1}{\alpha^2} = \left(\frac{e^{-2i\kappa-\mathcal{H}(\zeta)}+1}{e^{-2i\kappa-\mathcal{H}(\zeta)}-1}\right)\left(\frac{e^{\mathcal{H}(\zeta)}+1}{e^{\mathcal{H}(\zeta)}-1}\right) = \frac{\cos\kappa+\cos(\kappa-i\mathcal{H}(\zeta))}{\cos\kappa-\cos(\kappa-i\mathcal{H}(\zeta))}. \tag{A11}$$

But,

$$\frac{1}{\alpha^2} = -\frac{1}{r^2} = -\cot^2(\Phi/4) = -\frac{\cos^2(\Phi/4)}{\sin^2(\Phi/4)} = \frac{\cos(\Phi/2)+1}{\cos(\Phi/2)-1}, \tag{A12}$$

where, in the last step, (45) has been used, and familiar trigonometric identities. On comparison of (A11) and (A12), it is clear that

$$\frac{\cos\kappa}{\cos(\kappa-i\mathcal{H}(\zeta))} = \cos(\Phi/2), \quad \text{or} \quad \kappa - i\mathcal{H}(\zeta) = \cos^{-1}\left(\frac{\cos\kappa}{\cos(\Phi/2)}\right). \tag{A13}$$

The result (59) follows from combining (A1) and (A13).

[1] A. Zöttl and H. Stark, Emergent behavior in active colloids, J. Phys.: Condens. Matter **28**, 253001 (2016).

[2] N. J. Suematsu and S. Nakata, Evolution of self-propelled objects: From the viewpoint of nonlinear science, Chem. Eur. J. **24**, 6308 (2018).

[3] S. Nakata, M. Nagayama, H. Kitahata, N. J. Suematsu, and T. Hasegawa, Physicochemical design and analysis of self-propelled objects that are characteristically sensitive to environments, Phys. Chem. Chem. Phys. **17**, 10326 (2015).

[4] C. H. Meredith, A. C. Castonguay, Y.-J. Chiu, A. Sen, D. Velegol, and L. D. Zarzar, Chemical design of self-propelled Janus droplets, Matter **5**, 616 (2022).

[5] H. Su, S. Li, G.-Z. Yang, and K. Qian, Janus micro/nanorobots in biomedical applications, Adv. Healthcare Mater. **12**, 2202391 (2023).

[6] S. Sanchez, L. Soler, and J. Katuri, Chemically powered micro- and nanomotors, Angew. Chem. Int. Ed **54**, 1414 (2015).

[7] R. Golestanian, T. B. Liverpool, and A. Ajdari, Designing phoretic micro-and nano-swimmers, New J. Phys. **9**, 126 (2007).

[8] S. Michelin, Self-propulsion of chemically active droplets, Annu. Rev. Fluid Mech. **55**, 77 (2023).

[9] W. F. Paxton, K. C. Kistler, C. C. Olmeda, A. Sen, S. K. S. Angelo, Y. Cao, T. E. Mallouk, P. E. Lammert, and V. H. Crespi, Catalytic nanomotors: Autonomous movement of striped nanorods, J. Am. Chem. Soc. **126**, 13424 (2004).

[10] S. Ebbens, M.-H. Tu, J. R. Howse, and R. Golestanian, Size dependence of the propulsion velocity for catalytic janus-sphere swimmers, Phys. Rev. E **85**, 020401(R) (2012).

[11] J. Happel and H. Brenner, *Low Reynolds Number Hydrodynamics* (Springer, Dordrecht, 1983).

[12] D. G. Crowdy, Wall effects on self-diffusiophoretic Janus particles: A theoretical study, J. Fluid Mech. **735**, 473 (2013).

[13] D. Sondak, C. Hawley, S. Heng, R. Vinsonhaler, E. Lauga, and J-L Thiffeault, Can phoretic particles swim in two dimensions, Phys. Rev. E **94**, 062606 (2016).
[14] E. Yariv and D. G. Crowdy, Phoretic self-propulsion of Janus disks in the fast-reaction limit, Phys. Rev. Fluids **5**, 112001(R) (2020).
[15] W.-F. Hu, T.-S. Lin, S. Rafai, and C. Misbah, Chaotic swimming of phoretic particles, Phys. Rev. Lett. **123**, 238004 (2019)
[16] G. Li, Swimming dynamics of a self-propelled droplet, J. Fluid Mech. **934**, A20 (2022).
[17] G. Zhu and L. Zhu, Self-propulsion of an elliptical phoretic disk emitting solute uniformly, J. Fluid Mech. **974**, A57 (2023).
[18] D. G. Crowdy, Exact solutions for cylindrical "slip-stick" Janus swimmers in Stokes flow, J. Fluid Mech. **719**, R2 (2013).
[19] J. W. M. Bush and D. L. Hu, Walking on water: Biolocomotion at the interface, Annu. Rev. Fluid Mech. **38**, 339 (2006).
[20] K. Dietrich, N. Jaensson, I. Buttinoni, G. Volpe, and L. Isa, Microscale Marangoni surfers, Phys. Rev. Lett. **125**, 098001 (2020).
[21] A. Würger, Thermally driven Marangoni surfaces, J. Fluid Mech. **752**, 589 (2014).
[22] E. Lauga and A. M. J. Davis, Viscous Marangoni propulsion, J. Fluid Mech. **705**, 120 (2012).
[23] D. G. Crowdy, Collective viscous propulsion of a two-dimensional flotilla of Marangoni boats, Phys. Rev. Fluids **5**, 124004 (2020).
[24] J. R. Philip, Flows satisfying mixed no-slip and no-shear conditions, J. Appl. Math. Phys. **23**, 353 (1972).
[25] D. G. Crowdy, Frictional slip lengths for unidirectional superhydrophobic grooved surfaces, Phys. Fluids **23**, 072001 (2011).
[26] K. H. Nagai, F. Takavbatake, Y. Sumino, H. Kitahata, M. Ichikawa, and N. Yoshinaga, Rotational motion of a droplet induced by interfacial tension, Phys. Rev. E **87**, 013009 (2013).
[27] E. Lauga, W. R. DiLuzio, G. M. Whitesides, and H. A. Stone, Swimming in circles: Motion of bacteria near solid boundaries, Biophys. J. **90**, 400 (2006).
[28] E. Yariv and M. Siegel, Rotation of a superhydrophobic cylinder in a viscous liquid, J. Fluid Mech. **880**, R4 (2019).
[29] M. Siegel and E. Yariv, Jeffery's paradox for the rotation of a single 'stick–slip' cylinder, Mech. Res. Commun. **131**, 104154 (2023).
[30] D. G. Crowdy, Torque-driven superhydrophobic cylinders swim in circles, Proc. Roy. Soc. A **480**, (2024).
[31] H. Wong, D. Rumschitzki, and C. Maldarelli, On the surfactant mass balance at a deforming fluid interface, Phys. Fluids **8**, 3203 (1996).
[32] W. E. Langlois and M. O. Deville, *Slow Viscous Flows*, 2nd ed. (Springer, New York, 2014).
[33] D. G. Crowdy, Conformal slit maps in applied mathematics, ANZIAM Journal **53**, 171 (2012).
[34] D. G. Crowdy, Solving problems in multiply connected domains, *CBMS-NSF Regional Conference Series in Applied Mathematics* (Society for Industrial and Applied Mathematics, Philadelphia, 2020).